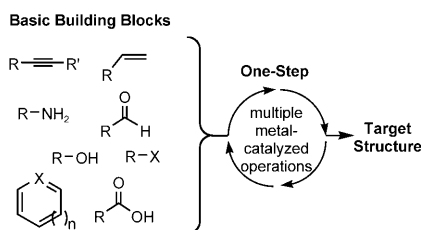


CONCEPTS

Transition-Metal Catalysts

*B. A. Arndtsen** 302–313

Metal-Catalyzed One-Step Synthesis: Towards Direct Alternatives to Multi-step Heterocycle and Amino Acid Derivative Formation



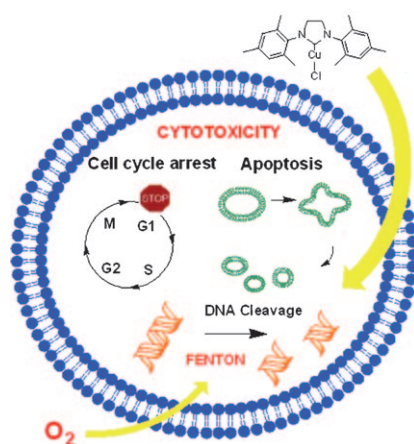
All at once: The reactivity of transition-metal catalysts can be exploited to design one-step methods to convert readily available building blocks directly into a diverse array of products (see scheme). In contrast with multistep syntheses, these rely upon multiple catalytic operations occurring in sequence to build up these structures.

COMMUNICATIONS

Anticancer Agents

M.-L. Teyssot, A.-S. Jarrousse, A. Chevy, A. De Haze, C. Beaudoin, M. Manin, S. P. Nolan, S. Díez-González, L. Morel, A. Gautier** 314–318

Toxicity of Copper(I)–NHC Complexes Against Human Tumor Cells: Induction of Cell Cycle Arrest, Apoptosis, and DNA Cleavage

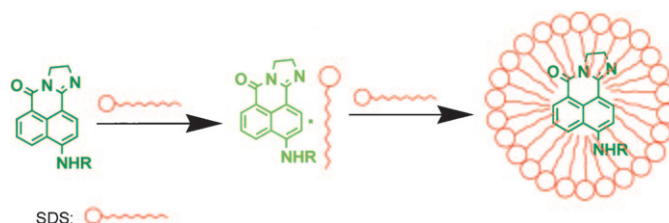


Tumor cell killer: Copper(I)–NHC [CuCl(SIMes)] shows high cytotoxicity against human cancer cells. An increase of up to 150 fold compared with cisplatin was observed. The complex causes arrest of the cell cycle progression at the G1 phase concomitantly with apoptosis induction at low concentration (see scheme). This copper(I)–NHC also produces DNA strand breaks, which demonstrates its value as a Fenton-like reagent.

Sensors

J. Qian, X. Qian, Y. Xu* 319–323

Selective and Sensitive Chromo- and Fluorogenic Dual Detection of Anionic Surfactants in Water Based on a Pair of “On–Off–On” Fluorescent Sensors



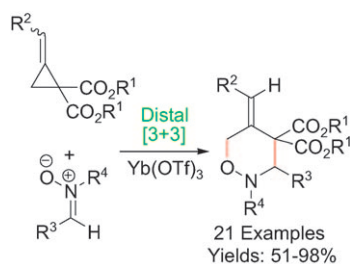
An “on-off-on” fluorescent sensor was used to sense anionic surfactant SDS with high sensitivity and selectivity due to the formation of 1:1 complex with SDS. The detection range can be adjusted by altering the substituting

alkyl chain length (NHR in the figure). The sensor array can discriminate not only anionic surfactant SDS, but also its concentration ranges from other species.

[3+3] Cycloaddition

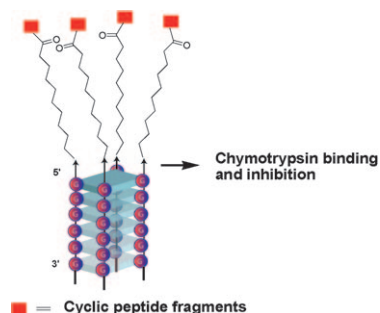
*B. Hu, J. Zhu, S. Xing, J. Fang, D. Du, Z. Wang** 324–327

A Highly Site-, Regio-, and Stereoselective Lewis Acid Catalyzed Formal [3+3] Cycloaddition of Methylene-cyclopropane-1,1-Diesters with C,N-Diarylnitrones



Another pathway: A new type of Lewis acid promoted [3+3] cycloaddition of methylenecyclopropane-1,1-diester with C,N-diarylnitrones is disclosed. This cycloaddition is highly site-, regio-, and stereoselective and proceeds in moderate-to-excellent yields. A three-component one-pot version of the cycloaddition is also reported.

A novel family of synthetic receptors was prepared for protein-surface recognition. The inhibition of chymotrypsin was achieved through protein-surface binding by four peptide loops arrayed on a DNA quadruplex scaffold (see figure). The most potent identified inhibitor has a $K_i^{app} = 0.33 \mu\text{M}$. Detailed kinetic analysis revealed a two-step slow binding inhibition mechanism for the inhibition of ChT by this inhibitor.



Synthetic Receptors

*J. Cai, B. A. Rosenzweig, A. D. Hamilton** 328–332

Inhibition of Chymotrypsin by a Self-Assembled DNA Quadruplex Functionalized with Cyclic Peptide Binding Fragments



Look—no transition metal! Transition-metal-free systems for the direct cross-coupling reactions of nitrogen heteroaromatics and alkanes are described. Under the influence of *t*BuOO*t*Bu,

pyridine *N*-oxide derivatives react with alkanes to furnish the corresponding cross-coupling products (alkylated nitrogen heterocycles) in good yields.

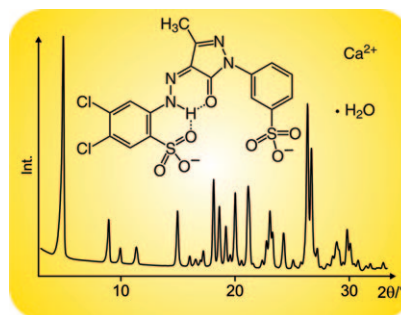
Cross-Coupling Reactions

G. Deng, K. Ueda, S. Yanagisawa, K. Itami, C.-J. Li** 333–337

Coupling of Nitrogen Heteroaromatics and Alkanes without Transition Metals: A New Oxidative Cross-Coupling at C–H/C–H Bonds



For more than 100 years, laked azo pigments (i.e., dyestuff anions combined with M^{2+} cations) have been industrially produced, but crystal structures of commercial laked pigments have never been reported. The crystal structures of two such pigments were determined from laboratory X-ray powder data (see graphic).



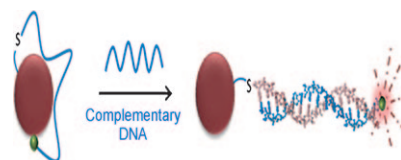
Dyes and Pigments

M. U. Schmidt, J. van de Streek, S. N. Ivashevskaya* 338–341

The First Crystal Structures of Industrial Laked Yellow Pigments Determined by X-ray Powder Diffraction



Size matters! This article demonstrates for the first time that size- and distance-dependent nanoparticle surface-energy transfer (NSET) properties of gold nanoparticles can be used for recognizing hepatitis C virus RNA sequences (see scheme) sensitively (300 fM concentration) and selectively (single-base mutations) in a homogeneous format.



FULL PAPERS

Gold Nanoparticles

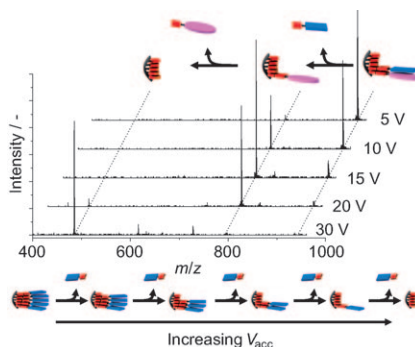
*J. Griffin, A. K. Singh, D. Senapati, P. Rhodes, K. Mitchell, B. Robinson, E. Yu, P. C. Ray** 342–351

Size- and Distance-Dependent Nanoparticle Surface-Energy Transfer (NSET) Method for Selective Sensing of Hepatitis C Virus RNA

DNA Hybrids

P. G. A. Janssen, J. L. J. van Dongen,
E. W. Meijer,*
A. P. H. J. Schenning* 352–360

 **Electrospray-Ionization Mass Spectrometry for Screening the Specificity and Stability of Single-Stranded-DNA Templated Self-Assemblies**

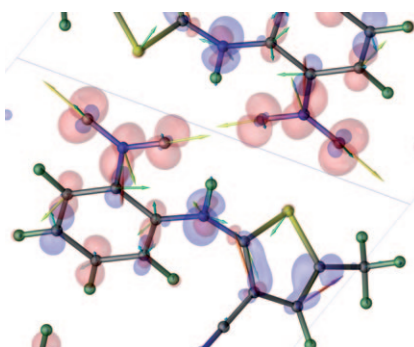


A complex break up: Supramolecular complexes consisting of a single-stranded oligothymine as the host template and an array of guests molecules equipped with a complementary diaminotriazine hydrogen-bonding unit have been studied with electrospray-ionization mass spectrometry and collision-induced-dissociation experiments (see spectra; V_{acc} : acceleration voltage).

Crystal Packing

T. Li,* P. W. Ayers, S. Liu,
M. J. Swadley,
C. Aubrey-Medendorp 361–371

Crystallization Force—A Density Functional Theory Concept for Revealing Intermolecular Interactions and Molecular Packing in Organic Crystals

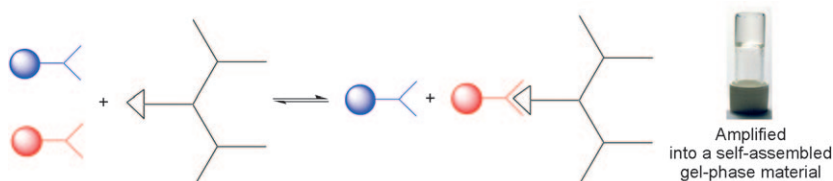


It's the electron! Polymorphism of organic crystals presents a significant challenge for theoretical chemists to develop methods and tools predicting crystal structures of a given compound. The electronic concept “crystallization force” characterizes the locality of intermolecular interactions in a crystal (see figure) and may provide a means to understand and calculate molecular-packing structures.

Self-Assembly

A. R. Hirst, J. F. Miravet, B. Escuder,
L. Noirez, V. Castelletto, I. W. Hamley,
D. K. Smith* 372–379

Self-Assembly of Two-Component Gels: Stoichiometric Control and Component Selection



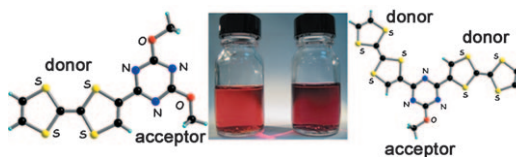
Two-component gels based on a combination of a L-lysine-based dendron and a rigid diamine spacer (1,4-diaminobenzene or 1,4-diaminocyclohexane) are investigated (see figure). The gels spontaneously self-organise in a com-

ponent-selective manner, with the dendron preferentially recognising 1,4-diaminobenzene and amplifying this building block in the immobilised gel-phase network when similar competitor diamines are present.

Donor–Acceptor Systems

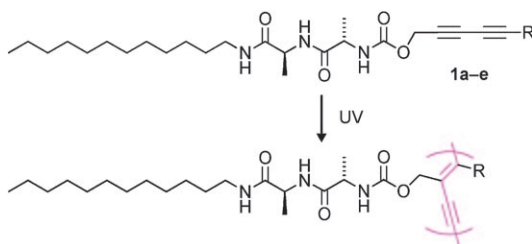
F. Riobé, P. Grosshans,
H. Sidorenkova, M. Geoffroy,*
N. Avarvari* 380–387

 **Mono- and Bis(tetrathiafulvalene)-1,3,5-Triazines as Covalently Linked Donor–Acceptor Systems: Structural, Spectroscopic, and Theoretical Investigations**



New covalently linked (multi)donor acceptor systems (shown here) were formed by reaction of 2,4,6-trichloro-1,3,5-triazine with lithiated tetrathiafulvalene (TTF), followed by treatment with sodium methanolate to pro-

vide mono- and bis(TTF)–triazines. They have planar solid-state structures, for which intramolecular charge transfer is evidenced and the radical oxidized species analyzed by EPR spectroscopy.



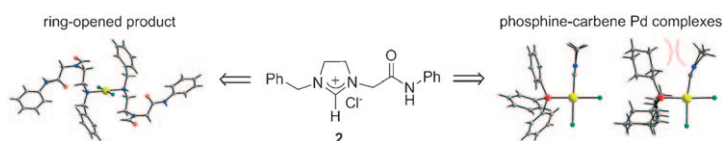
Self-organization: A series of peptide-containing amphiphilic diacetylenes **1a–e** was prepared and used to investigate the role of N–H···O=C hydrogen-

bonding sites and the hydrophobic moiety in their self-organization in organic solvents as well as their topochemical polymerizability.

Self-Assembly

*E. Jahnke, J. Weiss, S. Neuhaus, T. N. Hoheisel, H. Frauenrath** 388–404

Synthesis of Diacetylene-Containing Peptide Building Blocks and Amphiphiles, Their Self-Assembly and Topochemical Polymerization in Organic Solvents



The imidazolium salt **2** is very sensitive to moisture and can undergo ring-opening reactions very readily. Pd^{II} complexes with the ring-opened products from imidazolium salts were isolated and characterized by X-ray crys-

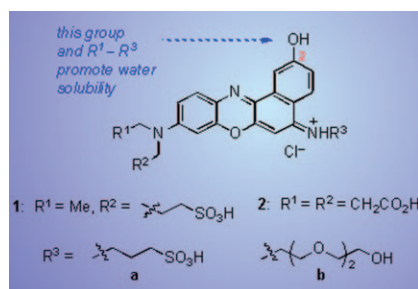
tallography. Robust and electron-rich mixed phosphine/carbene Pd^{II} complexes were successfully prepared that display competent coupling activities (see figure).

Cross-Coupling

*C.-Y. Liao, K.-T. Chan, C.-Y. Tu, Y.-W. Chang, C.-H. Hu, H. M. Lee** 405–417

Robust and Electron-Rich *cis*-Palladium(II) Complexes with Phosphine and Carbene Ligands as Catalytic Precursors in Suzuki Coupling Reactions

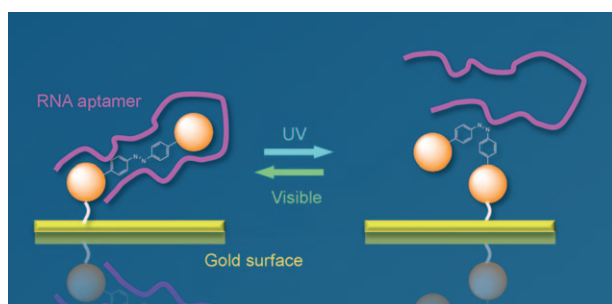
That's why they call it the blues! Water-soluble Nile Blue derivatives **1a,b** and **2a,b** (see scheme) have been prepared under mild conditions, and show superior quantum yields and sharper fluorescence emissions compared with other known water-soluble Nile Blue derivatives. Additionally, compounds **1** and **2** do not aggregate at low concentrations and show promise as biomolecule labels.



Benzophenoxazinium Dyes

*J. Jose, Y. Ueno, K. Burgess** 418–423

Water-Soluble Nile Blue Derivatives: Syntheses and Photophysical Properties



Photoregulation of binding between a peptide–ligand and its RNA aptamers was demonstrated by surface plasmon resonance (SPR) measurements. Furthermore, combinatorial use of an

RNA secondary structure prediction program and the doped reselection method provided a plausible structure of the selected RNA aptamer.

RNA Aptamers

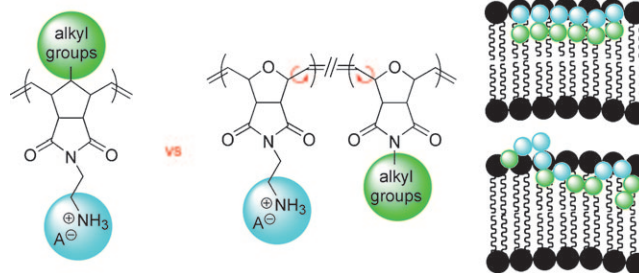
*G. Hayashi, M. Hagihara, K. Nakatani** 424–432

RNA Aptamers That Reversibly Bind Photoresponsive Azobenzene-Containing Peptides

Amphiphilic Polymers

G. J. Gabriel, J. A. Maegerlein,
C. F. Nelson, J. M. Dabkowski, T. Eren,
K. Nüsslein, G. N. Tew* 433–439

Comparison of Facially Amphiphilic versus Segregated Monomers in the Design of Antibacterial Copolymers



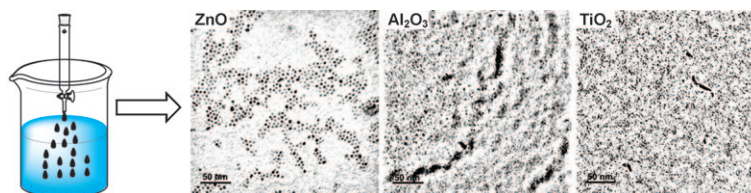
Striking a balance between hydrophobic and hydrophilic groups is essential for antibacterial polymers to interact and disrupt bacterial membranes (see figure). A more detailed strategy, beyond varying polymer amphiphilic-

ity, remains elusive though. The differences in properties of polymers obtained by two fundamentally distinct routes reported here are quite significant and worthy of investigation.

Nanoparticles

L. Chen, J. Xu, D. A. Tanner,
R. Phelan, M. Van der Meulen,
J. D. Holmes, M. A. Morris* .. 440–448

One-Step Synthesis of Stoichiometrically Defined Metal Oxide Nanoparticles at Room Temperature



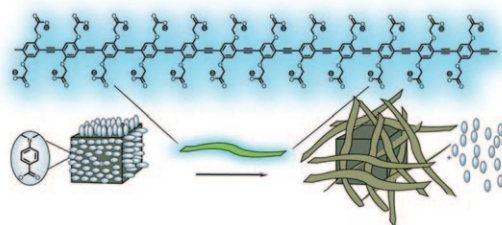
Metathesis of metal oxides occurs between two types of metal oxides, that is, it is transferred from one oxide to another in which the more soluble one acts as an oxide anion source and

the less soluble one forms the product. This methodology provides a novel route to produce nanoscale oxide materials (see picture) in an inexpensive and highly efficient way.

Fluorescence Probe

I.-B. Kim, M. H. Han, R. L. Phillips,
B. Samanta, V. M. Rotello, Z. J. Zhang,
U. H. F. Bunz* 449–456

Nano-Conjugate Fluorescence Probe for the Discrimination of Phosphate and Pyrophosphate



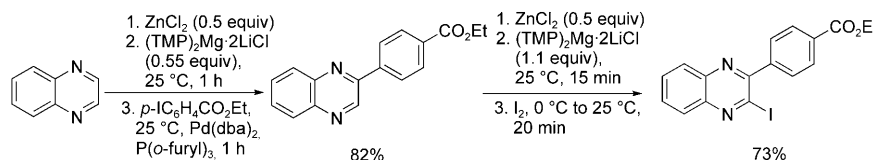
A bio-analytical probe? A pyrophosphate (PPi) probe is described that is based on a fluorescent dicarboxylate-substituted poly(*para*-phenylene-

ethynylene) (PPE) and 10 nm cobalt-iron spinel nanoparticles (NPs) in aqueous media (see scheme).

Metalation

Z. Dong, G. C. Clososki,
S. H. Wunderlich, A. Unsinn, J. Li,
P. Knochel* 457–468

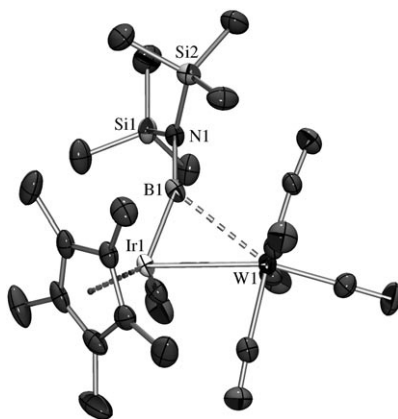
Direct Zincation of Functionalized Aromatics and Heterocycles by Using a Magnesium Base in the Presence of ZnCl₂



Power base! A wide range of polyfunctional aryl and heteroaryl zinc reagents were efficiently prepared in THF by using (TMP)₂Mg·2LiCl in the presence of ZnCl₂ (TMP = 2,2,6,6-tetramethylpi-

peramidyl; see scheme). The protocol allows tolerance of functional groups and efficient zincation of sensitive heterocycles such as quinoxaline.

Photochemically induced borylene transfer to $[(\eta^5\text{-C}_5\text{R}_5)\text{M}(\text{CO})_2]$ ($\text{M} = \text{Rh}$, $\text{R} = \text{H}$; $\text{M} = \text{Ir}$, $\text{R} = \text{Me}$) from $[(\text{OC})_5\text{M}=\text{BN}(\text{SiMe}_3)_2]$ ($\text{M} = \text{Cr}$, W) generates the first instances of heterodinuclear bridged rhodium and iridium borylene complexes. The iridium borylene complexes feature an unprecedented coordination mode of the borylene ligand (see picture). Furthermore, the first heterodinuclear bridged borylene compound containing a chromium atom in the three-membered ring is presented.

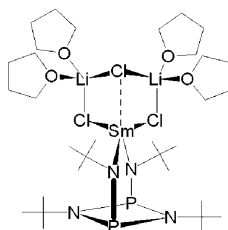


Boron Chemistry

H. Braunschweig, M. Forster, F. Seeler* 469–473

Synthesis and Structure of Heterodinuclear Rhodium and Iridium Borylene Complexes

Rare-earth cages: The first cyclodiphosph(III)azane complexes of the rare-earth elements have been synthesized. Thus, the metalate complexes of the composition $[\text{Li}(\text{thf})_4][\{(t\text{BuNP})_2(t\text{BuN})_2\}\text{LnCl}_3]$ and $[\{(t\text{BuNP})_2(t\text{BuN})_2\}\text{SmCl}_3\text{Li}_2(\text{thf})_4]$ (see scheme) were obtained. Heating of the lithium-containing complexes resulted in the neutral metal chloride complexes of the composition $[(t\text{BuNP})_2(t\text{BuN})_2\text{LnCl}(\text{thf})_2]$.

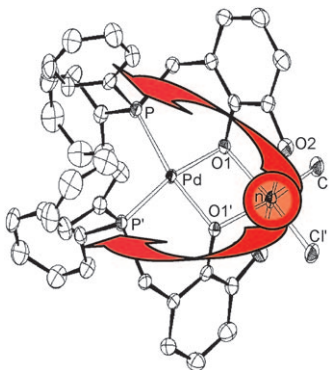


N,P Ligands

M. Rastätter, R. B. Muterle, P. W. Roesky, S. K.-H. Thiele* 474–481

Bis(amido)cyclodiphosph(III)azane Complexes of Yttrium and the Lanthanides

Tunable catalysts: Three-component reactions between a ditopic catechol phosphine ligand, a Pd salt, and a main group element or transition metal chloride yield—in a one-step fashion—heterobi- or trimetallic aggregates that can be described as Pd complexes with supramolecular bisphosphine ligands (see figure).

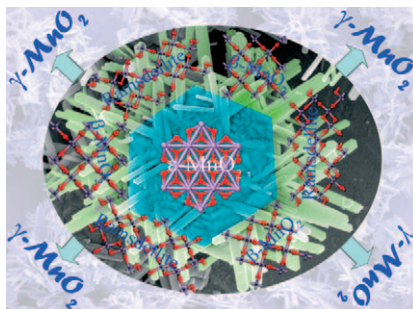


Palladium Complexes

S. H. Chikkali, D. Gudat, F. Lissner, M. Niemeyer, T. Schleid, M. Nieger* 482–491

Template-Controlled Assembly of Ditopic Catechol Phosphines: A Strategy for the Generation of Complexes of Bidentate Phosphines with Different Bite Angles

Where does the hexagonal symmetry come from? From the structural analysis of hexagon-based nanoarchitectures, the well-known “ $\gamma\text{-MnO}_2$ phase” was found to be metastable, heterogeneous phase assembly made up of akhtenskite ($\epsilon\text{-MnO}_2$), pyrolusite ($\beta\text{-MnO}_2$), and ramsdellite (see figure).



MnO₂ Nanostructures

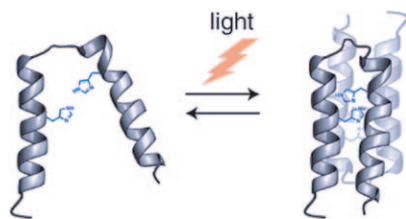
*C. Wu, W. Xie, M. Zhang, L. Bai, J. Yang, Y. Xie** 492–500

Environmentally Friendly $\gamma\text{-MnO}_2$ Hexagon-Based Nanoarchitectures: Structural Understanding and Their Energy-Saving-Applications

Peptidomimetics

*N. J. V. Lindgren, M. Varedian, A. Gogoll** 501–505

 **Photochemical Regulation of an Artificial Hydrolase by a Backbone Incorporated Tertiary Structure Switch**

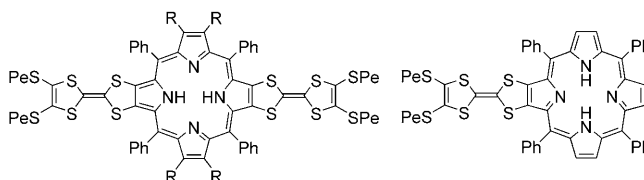


Toggle the tertiary structure: Photo-modulation of a chromophore in the backbone of a large catalytically active peptide is shown to change the aggregation of the peptide (see figure), thus affecting the rate of hydrolysis of an activated ester.

Porphyrins

K. A. Nielsen, E. Levillain, V. M. Lynch, J. L. Sessler, J. O. Jeppesen** 506–516

 **Tetrathiafulvalene Porphyrins**



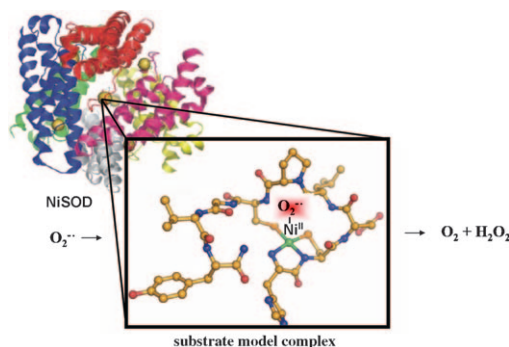
Communication between subunits is evident in functionalized porphyrins based on a tetraphenylporphyrin core onto which one (scheme, right), two (scheme, left), or four tetrathiafulvalene (TTF) subunits were annulated. Electron transfer from the TTF units

to the porphyrin chromophore occurs in the excited state(s) generated upon photoexcitation and, for the bis-TTF-annulated porphyrin, the two TTF units can communicate electronically through the intervening porphyrin.

Enzyme Catalysis

*D. Tietze, H. Breitzke, D. Imhof, E. Kothe, J. Weston, G. Buntkowsky** 517–523

New Insight into the Mode of Action of Nickel Superoxide Dismutase by Investigating Metallopeptide Substrate Models



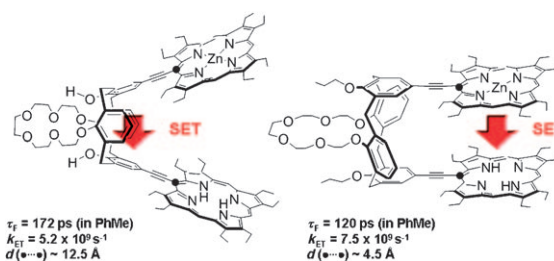
SOD adducts: For the first time, a stable substrate adduct of a nickel superoxide dismutase (NiSOD) model is isolated and its existence is proven by IR, UV/Vis, and liquid- and solid-

state NMR spectroscopy. This complex sheds new light on the question of whether the mode of action of the NiSOD enzyme (see structure) is an inner- or outer-sphere mechanism.

Singlet Energy Transfer

G. Pognon, J. A. Wytko, P. D. Harvey, J. Weiss** 524–535

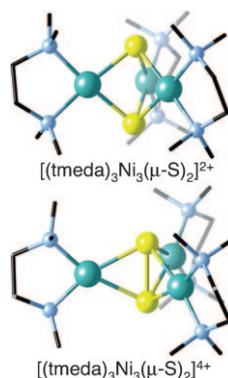
 **Evidence for Dual Pathway in Through-Space Singlet Energy Transfers in Flexible Cofacial Bisporphyrin Dyads**



The shortest pathway may not be a straight line for singlet energy transfer between a zinc porphyrin donor and a

free-base porphyrin, as through-space communication within a calixarene spacer can be observed (see scheme).

Count me in: The framework electron-counting rules presented for doubly bridged M_3X_2 cores in the $[(L_nM)_3X_2]$ trinuclear complexes depicted ($n = 2$ or 5), based on a qualitative molecular orbital analysis, are supported by density functional calculations (see figure, tmeda: tetramethylethylenediamine).



Through-Cage Bonding

*R. Carrasco, G. Aullón,
S. Alvarez** 536–546

**X–X Through-Cage Bonding in Cu,
Ni, and Cr Complexes with M_3X_2
Cores (X = S, As)**



* Author to whom correspondence should be addressed

Supporting information on the WWW (see article for access details).

Full Papers labeled with this symbol have been judged by two referees as being “very important papers”.

A video clip is available as Supporting Information on the WWW (see article for access details).

SERVICE

Spotlights _____ 298 Authors _____ 548 Keywords _____ 549 Preview _____ 551

Issue 1/2008 was published online on December 18, 2008



Fast, Individual, Popular...
REPRINTS
Available to order anytime!
Contact Carmen Leitner (e-mail: chem-reprints@wiley-vch.de)